Cellulose Nanofibril Hydrogel Promotes Hepatic Differentiation of Human Liver Organoids

Melanie Krüger, Loes A. Oosterhoff, Monique E. van Wolferen, Simon A. Schiele, Andreas Walther, Niels Geijsen, Laura De Laporte, Luc J. W. van der Laan, Linda M. Kock, and Bart Spee*

To replicate functional liver tissue in vitro for drug testing or transplantation, 3D tissue engineering requires representative cell models as well as scaffolds that not only promote tissue production but also are applicable in a clinical setting. Recently, adult liver-derived liver organoids are found to be of much interest due to their genetic stability, expansion potential, and ability to differentiate toward a hepatocyte-like fate. The current standard for culturing these organoids is a basement membrane hydrogel like Matrigel (MG), which is derived from murine tumor material and apart from its variability and high costs, possesses an undefined composition and is therefore not clinically applicable. Here, a cellulose nanofibril (CNF) hydrogel is investigated with regard to its potential to serve as an alternative clinical grade scaffold to differentiate liver organoids. The results show that its mechanical properties are suitable for differentiation with overall, either equal or improved, functionality of the hepatocyte-like cells compared to MG. Therefore, and because of its defined and tunable chemical definition, the CNF hydrogel presents a viable alternative to MG for liver tissue engineering with the option for clinical use.

1. Introduction

Liver diseases were the 12th leading cause of death in the United States in 2015 and the numbers are increasing.[1] Reasons for this high mortality include a lack of good treatments, a shortage of donor livers for transplantation, and a lack of knowledge about underlying pathologies.[2] The aim of liver tissue engineering is to develop three-dimensional (3D) liver tissues that replicate the in vivo liver functions as close as possible.[3] Successful liver constructs can on one hand side serve as a testing platform for xenobiotics, toxins, or as disease models.[4] On the other side, they can be used in vivo as an alternative for donor organs and as a basis for stimulating liver regeneration through cell delivery.[4]

Considering that one of the most significant causes for an acute liver failure (ALF) are drug-induced liver injuries (11% of all ALF cases in the United States),[5] there is a clear need for preclinical drug testing models that can accurately predict the effect of drugs on the liver tissue and improve the success rate of only 10% in clinical drug testing.[6] Current tissue-engineered liver models have significant disadvantages that hamper their use. Presently, the gold standard to test toxicity and metabolism consists of primary human hepatocyte cultures in 2D. However, 2D cultures fail to represent the complex 3D structure of native liver tissue[7] and further problems associated with primary hepatocytes are limited availability, restricted lifespan, rapid dedifferentiation, functional variability, and a limit in drug transporter

M. Krüger, L. A. Oosterhoff, M. E. van Wolferen,
Prof. N. Geijsen, Dr. B. Spee
Department of Clinical Sciences of Companion Animals
Faculty of Veterinary Medicine
Utrecht University
Uppsalalaan 8, 3584 CT Utrecht, The Netherlands
E-mail: b.spee@uu.nl
M. Krüger, Dr. L. M. Kock
LifeTec Group BV
Kennedyplein 10-11, 5611 ZS Eindhoven, The Netherlands

The ORCID identification number(s) for the author(s) of this article can be found under https://doi.org/10.1002/adhm.201901658.

S. A. Schiele
Prof. L. De Laporte
DWI – Leibniz-Institut für Interaktive Materialien e.V.
Advanced Materials for Biomedicine
ITMC – Institute of Technical and Macromolecular Chemistry
RWTH University Aachen
Forckenbeckstr. 50, 52056 Aachen, Germany
Prof. A. Walther
Albert-Ludwigs-Universität Freiburg
Institute for Macromolecular Chemistry
Stefan-Meier-Strasse 3, Hermann Staudinger Building, 79104 Freiburg, Germany
Prof. N. Geijsen
Hubrecht Institute for Developmental Biology and Stem Cell Research
University Medical Center Utrecht
Uppsalalaan 8, 3584 CT Utrecht, The Netherlands
Prof. L. J. W. van der Laan
Department of Surgery
Erasmus MC
Postbus 2040, 3000 CA Rotterdam, The Netherlands

ADVANCED
SCIENCE NEWS
www.advancedsciencenews.com

ADVANCED
HEALTHCARE
MATERIALS
www.advhealthmat.de

activity.[8] Moreover, despite their large replication capacity in vivo, hepatocytes cannot be expanded in culture.[9] A predictive cell model, therefore, needs to have a stable hepatic signature and the potential to expand to be readily available,[9] and should be 3D.[8] For stem cell derived hepatocyte like cells or even adult hepatocytes, it is known that a 3D structure leads to an improved survival rate and functional phenotype.[10]

One of the potential solutions is using liver-derived adult stem cells cultured as organoids. These organoids create structures that resemble their organ of origin by assembling themselves into a 3D structure and growing and expanding in vitro.[11] Adult stem cells isolated from human liver biopsies can be cultured in a 3D extracellular matrix (ECM) mimicking the microenvironment of these cells in vivo.[11] Liver organoids allow for an almost infinite and genetically stable expansion of adult stem cells in vitro and can be differentiated into hepatocyte-like cells.[9] These organoids are maintained in Matrigel (MG), which is a thermosensitive hydrogel prepared from a basement membrane rich sarcoma, the Engelbreth–Holm–Swarm murine tumor, which must be propagated in mice.[12] Therefore, MG is a material of undefined murine origin with a high batch-to-batch variability of up to 50%[13] and high purchase costs.[12] For the liver organoids to be used in in vitro models or in the clinic, new hydrogels need to be tested that allow for a better hepatic differentiation, and provide a scaffold that can be applied clinically. For clinical application, it is essential for the material to have the potential for approval by the FDA or other regulatory bodies and comply with good manufacturing practices, which is not possible for MG, due to the animal origin and undefined composition.[3]

One potential alternative biomaterial for MG that is shear thinning, swellable in water, and enables 3D cell culture is cellulose, which is the most abundant biopolymer on earth with its main source being cell walls of plants.[14,15] In nature, cellulose is formed by micron-sized fibril agglomerations of diameters between 2 and 20 μm, depending on its source.[16] Extraction can be achieved through oxidation mediated by 2,2,6,6-tetramethylpiperidinyl-1-oxyl (TEMPO), which catalyzes the oxidation of primary alcohol groups in the presence of water.[16] In this way, aldehyde and carboxyl groups are introduced[17] on to the surface of the fibers[16] resulting in a negative surface charge which enables the subsequent separation of the fibrils[17] with a pressure homogenizer.[18] This results in nanofibrils with a thickness of 2.5 ± 2 nm that are very crystalline and have a high aspect ratio.[18] These fibrils, consisting of β-D glycopyranose polysaccharide chains[6] are one of the stiffest natural biomaterials with $E_{cellulose.I} = 138$ GPa and they are the underlying reason for the remarkable mechanical properties of the hydrogel.[18] When mixed with water, they form reversible cellulose nanofibril (CNF)[17] hydrogels already at very low solid contents[18] of ≈0.2%. The nanoscale network within this hydrogel can be seen in SEM images of the material.[19] The shear-thinning and self-healing behavior associated with this hydrogel[18] is due to the entanglement, hydrogen bonds, and ionic interactions that keep it together,[17] which also prevent degradation in aqueous environments.[20] The CNF is naturally biocompatible[12,21] and has therefore been used for different tissue engineering applications. Among those with promising results are cultures in CNF hydrogel of stem cells,[12] culture,[6]

and differentiation[8] of liver cell lines such as HepaRG and HepG2 or progenitor cell thereof and as a sacrificial template for the engineering of tubular cell constructs.[19] The hydrogel is very stable in the long term and fabrication costs are much lower compared to other materials, such as MG.[20] CNFs are not degradable in humans,[14,22,23] but controlled degradation can be achieved by either adding the enzyme cellulase[12,22] or making use of the shear-thinning properties and reaching degradation through medium flow[24] if desired.
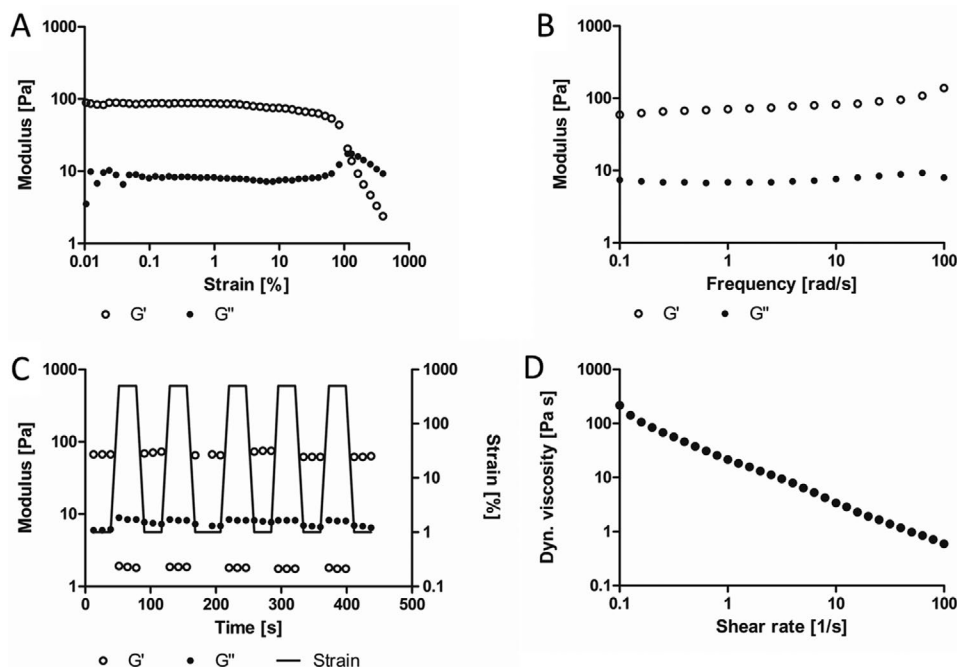
To our knowledge CNF hydrogels have only been tested in combination with cell lines, which are associated with the abovementioned drawbacks. Cellulose as a natural polymer in combination with human liver organoids would fulfil most of the significant characteristics necessary for successful liver tissue engineering mentioned in a recent review on the specific demands of hydrogels for this purpose.[3] These are namely the human autologous cell source, the potential to include vasculature, possible additions of bioactive substrates, biocompatibility, bioprintability, chemical definition, mechanical properties in the range of 0.2–1 kPa and the possibility to be degradable. Therefore, the aim of this study is to test the potential of CNF hydrogels as a scaffold for liver tissue engineering. For that purpose, human liver organoids from several donors were differentiated in CNF hydrogels and examined with respect to their metabolic activity, maturation level, functionality, and polarization in comparison to MG to assess the potential of CNF as a scaffold for differentiation of human liver organoids into functional hepatocytes for toxicity testing and regenerative medicine.

2. Results

2.1. Hydrogel Characterization

To examine the mechanical characteristics of the hydrogel, we have performed a rheological analysis by conducting an amplitude sweep measurement (**Figure 1**A), frequency sweep (Figure 1B), altering strain measurement (Figure 1C), and dynamic viscosity measurement (Figure 1D). As is visualized in Figure 1A, CNF hydrogel exhibits highly elastic behavior with G' (84.1 ± 4.2 Pa) roughly 10 times that of G'' (8 ± 0.4 Pa) before the critical strain point of about 100% strain. From the frequency sweep in Figure 1B, it can be observed that G' and G'' are nearly constant over the range of frequencies between 0.1 and 10 rad s^{-1} with $G' > G''$. Rapid self-healing is demonstrated by the altering strain experiment shown in Figure 1C. At high strains G'' is higher than G', but by altering back to low strain, the storage modulus G' recovers quickly, restoring the original viscoelastic property. Complete recyclability is shown by repeating this process over five cycles without a change in property. The CNF hydrogel also demonstrates shear-thinning behavior as can be seen in Figure 1D with a viscosity decrease for increasing shear rates. The Young's modulus (E) is calculated to be ≈255 Pa with a plateau value of G' of 85 Pa of the frequency sweep.

As can be seen in **Figure 2**, the swelling ratio of the CNF hydrogel in demineralized water increases by 17% (±7.5) after only 30 min, which reduces the cellulose concentration from 0.6% (w/v)

**ADVANCED
SCIENCE NEWS**

www.advancedsciencenews.com

**ADVANCED
HEALTHCARE
MATERIALS**

www.advhealthmat.de

Figure 1. Rheological data of 0.4 mL of 0.6% (w/v) cellulose nanofibril (CNF) hydrogel at 20 and a plate gap of 0.5 mm. A) Dynamic oscillatory amplitude sweep measurement at 1 rad s^{-1}. B) Frequency sweep measurements at 0.5% oscillating strain. C) Altering strain measurement between 1% and 500% in periods of 30 s. D) Dynamic viscosity measurement with 5 s equilibrium time and 30 s averaging time.

to 0.54% (w/v) (±0.04) and there is no equilibrium reached after 4 h. This is also the reason for the high standard deviations, as differentiation between the hydrogel and water is hardly possible after extended swelling times. This effect is not observed for swelling in phosphate buffered saline (PBS), where an equilibrium is reached after only 30 min.

2.2. . Morphology and Metabolic Activity

To test the potential of human liver organoids to expand within the CNF hydrogel, the organoids were reseeded into MG and CNF hydrogels and cultured for 7 days with expansion medium (EM). The Alamar Blue staining (Figure S1, Supporting Information) shows that there is no significant increase in metabolic activity
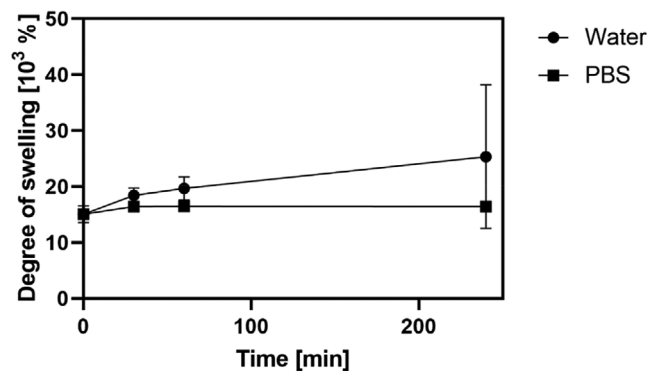

Figure 2. Degree of swelling for 0.5 mL 0.6% (w/v) cellulose nanofibril (CNF) hydrogel in 2 mL demineralized water and 1× PBS over 4 h, data depicted as mean ± SD ($n = 3$).

over the culture period within the CNF hydrogel, whereas the metabolic activity increases by 73% ($p = 0.0011$) in MG, which indicated that organoids cannot be propagated in CNF.

For assessing the differentiation potential, human liver organoids from three donors were expanded in MG before being transferred to another MG or to CNF. In MG, two different media conditions were compared—EM and differentiation medium (DM). In CNF hydrogel, only DM was used to show the differentiation potential of the biomaterial. In Figure S2, Supporting Information, it is shown that the metabolic activity within each day is not significantly different between any of the CNF hydrogel concentrations, therefore the data were averaged over all donors and CNF hydrogel concentrations and representative images are shown for morphology. When comparing CNF hydrogels to MG, more condensed, smaller, and darker human liver organoids were observed (**Figure 3**A). In the case of DM, the organoids did not appear to be proliferating in both MG and CNF hydrogel, while control samples cultured in MG with EM continued to grow over these 7 days. This was confirmed by the Alamar Blue staining, indicating that the total metabolic activity increases over time for organoids cultured in MG in EM up to 120% ($p = 0.0011$) on day 7 (Figure 3B). The organoids in MG and DM show no significant change in metabolic activity. In CNF hydrogel, an initial reduction of metabolic activity was observed for all donors with an average decrease of 23% ($p < 0.0001$) from days 1 to 4 but no significant difference between days 4 and 7.

2.3. Gene Expression

To determine the maturation level and fate of the hepatocyte-like cells after differentiation for 7 days in both CNF hydrogel

1901658 (3 of 12)
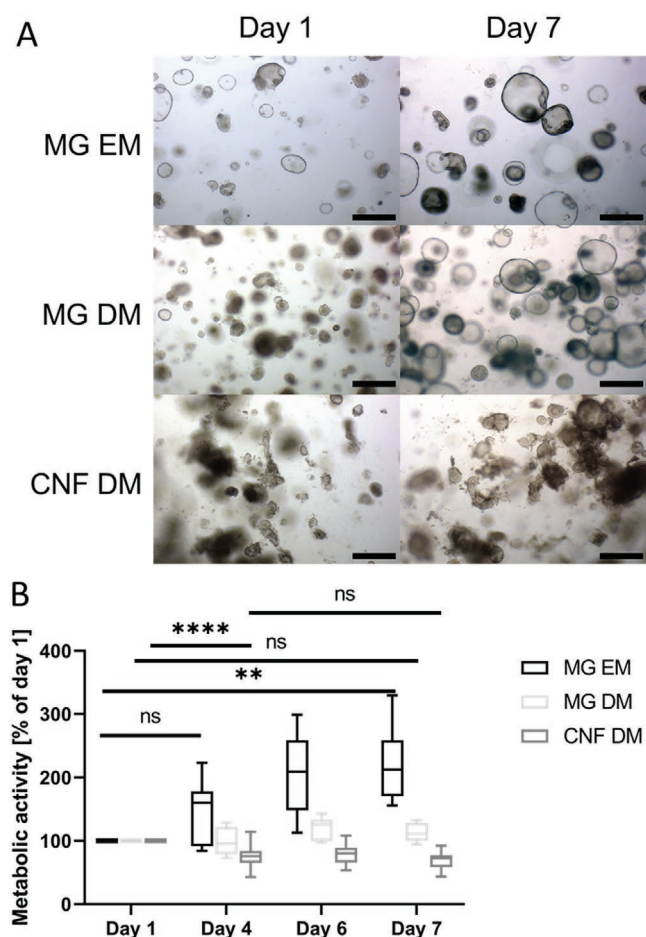
Figure 3. A) Representative brightfield images showing liver organoid morphology on days 1 and 7 after transfer into Matrigel (MG) under expansion medium (EM) or differentiation medium (DM) conditions, or in cellulose nanofibril (CNF) hydrogel 0.4% (w/v) under DM conditions, scale bar 500 µm. B) Metabolic activity at days 4, 6, and 7 relative to values at day 1 ($n = 9$ for MG EM and DM, $n = 24$ for CNF DM); data depicted as box with median and 25th and 75th percentile and whiskers from min to max (**$p < 0.01$, ****$p < 0.0001$, ns: not significant), ANOVA with Tukey's post-hoc test.

and MG, expression of genes was tested for DM and EM conditions. In Figure S3, Supporting Information, it is shown that gene expression is not statistically different between the great majority of the CNF concentrations, therefore the data were averaged over all cell donors and CNF conditions. For comparison, primary hepatocytes and a liver sample were analyzed simultaneously. Overall, expression levels of genes are always higher in DM compared to EM conditions, while in some cases the CNF hydrogel even outperforms MG. For example, expression levels of adult phase I specific enzymes, which belong to the cytochrome P450 family (CYP3A4, CYP1A2, CYP2D6, CYP2C19), demonstrate organoid functionality (**Figure 4,**). From these genes, CYP3A4 is expressed at 59% ($p = 0.0373$) higher levels in CNF DM compared to MG DM. For the phase II enzymes, UDP glucuronosyltransferase (UGT) (Figure 4K) and sulfotransferase (SULT) (Figure 4J), SULT presents a 32% ($p = 0.0205$) higher level of expression in the case of CNF DM over MG DM. Finally, phase III enzymes mitochondrial
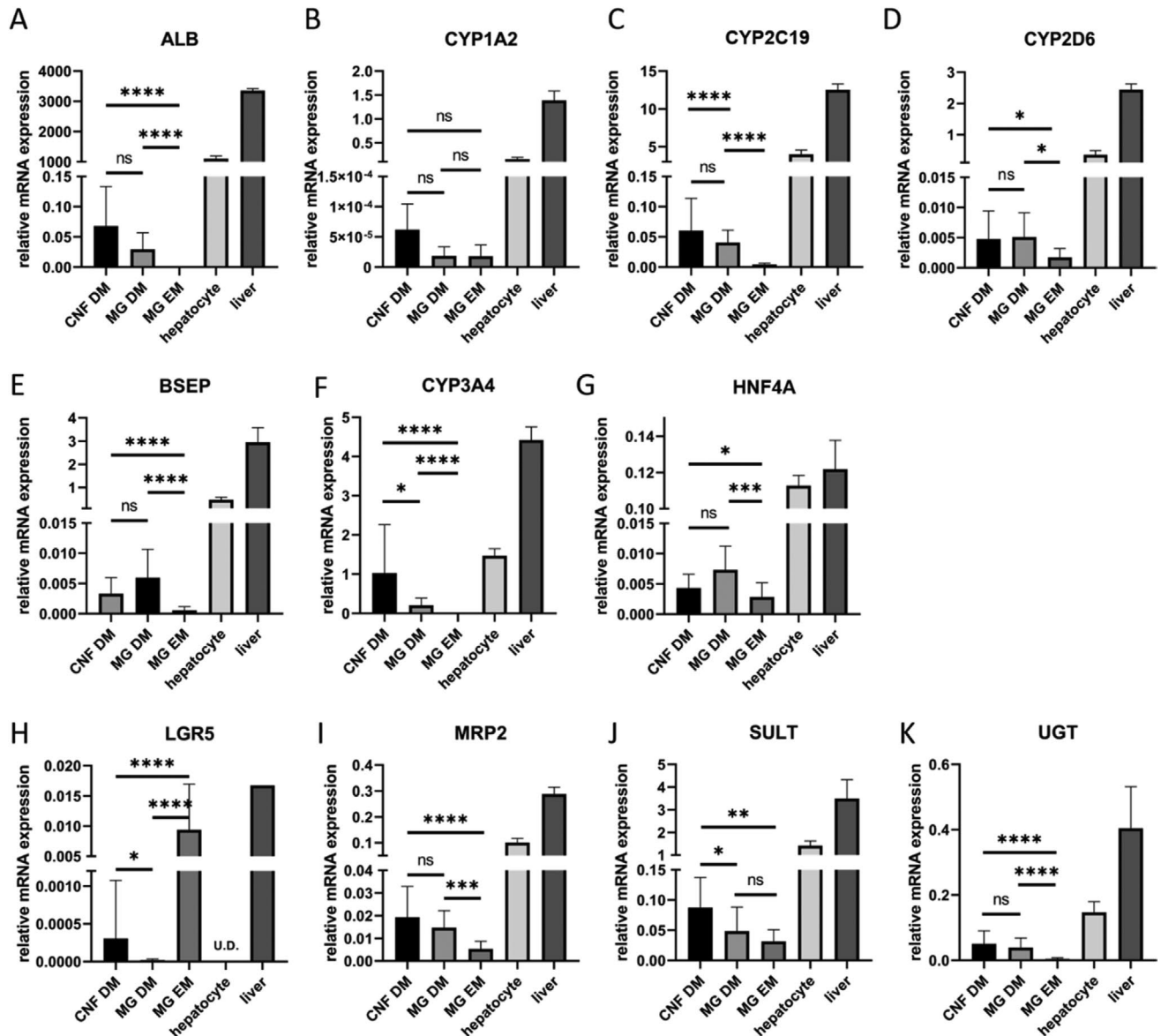
ribosomal protein S2 (MRP2) (Figure 4I) and ATP-binding cassette subfamily B member 11 (BSEP) (Figure 4E) both show no significant difference between organoids in CNF hydrogel or MG in DM. Only the stem cell marker leucine-rich repeat-containing G-protein coupled receptor 5 (LGR5), is expressed at significantly lower levels in both DM conditions (MG or CNF) compared to EM. Interestingly, some expression of this stem cell marker remained in CNF hydrogels (55%, $p = 0.0117$), while no expression was observed in MG with DM (Figure 4H).

2.4. Transaminase Activity

To further evaluate the performance of CNF hydrogels for differentiation of human liver organoid cultures in comparison to MG, the functionality of the hepatocyte-like cells was investigated by measuring the transaminase activity. For this purpose, cells were collected after 7 days of culture, where organoids in CNF hydrogels were differentiated with DM, whereas organoids in MG were cultured in both EM and DM, respectively. No significant differences between any CNF hydrogel concentrations (Figure S4, Supporting Information) results were observed and therefore data were averaged over donors and gel concentrations. Multiple hepatic markers were significantly higher in organoids under CNF DM conditions compared to MG DM conditions, such as alanine aminotransferase (ALAT) (28%, $p < 0.0001$) (**Figure 5**), aspartate transaminase (ASAT) (22%, $p = 0.009$), albumin production (85%, $p < 0.0001$), and glutamate dehydrogenase (GLDH) production (14%, $p = 0.0459$). Interestingly, ALAT enzyme, albumin, and GLDH production is not significantly different in MG when DM or EM is used. In contrast, organoids cultured in CNF hydrogel demonstrated higher levels of these differentiation signals compared to MG.

2.5. Immunocytology

For visualization and determination of specific expression sites, sections of the human liver organoids from all donors cultured in CNF hydrogel in DM or MG in DM or EM for 7 days, were stained immunocytochemically. Antibodies against the differentiation markers albumin, HNF4a, MRP2, tight junction protein, and polarization marker ZO1, as well as for glycogen accumulation with the Periodic acid–Schiff (PAS) stain were applied (**Figure 6**). The increase in albumin RNA levels in CNF hydrogels was confirmed by immunocytochemistry (Figure 6C), especially when compared to MG EM conditions (Figure 6A). The localization of albumin in MG is on the luminal side (Figure 6B), whereas it is on the apical side of the organoid in CNF. The early hepatocyte specification marker HNF4a is a transcription factor in the nuclei of organoids, therefore every staining outside the nuclei is unspecific. The specific nuclear staining can only be observed in CNF DM (Figure 6F) conditions, in MG EM and DM it is unspecific (Figure 6D,E). Another marker is MRP2, a protein expressed in the canalicular apical part of a hepatocyte that functions in biliary transport and therefore equally serves as a differentiation

ADVANCED
SCIENCE NEWS
www.advancedsciencenews.com

ADVANCED
HEALTHCARE
MATERIALS
www.advhealthmat.de

Figure 4. Relative gene expression to GAPDH and RPL19 of liver organoids differentiated in Matrigel (MG) and cellulose nanofibril (CNF) hydrogels (MG DM, CNF DM) for 7 days or cultured for 7 days in MG with EM (MG EM), with levels of native liver and hepatocytes as controls. Data are averaged over all CNF hydrogel concentrations (0.2–0.6% w/v) and donors. A) Albumin expression ($n = 15$ for MG EM, $n = 15$ for MG DM, $n = 39$ for CNF), B) CYP1A2 expression ($n = 4$ for MG EM, $n = 8$ for MG DM, $n = 21$ for CNF), C) CYP2C19 expression ($n = 15$ for MG EM, $n = 15$ for MG DM, $n = 39$ for CNF), D) CYP 2D6 expression ($n = 15$ for MG EM, $n = 15$ for MG DM, $n = 42$ for CNF), E) BSEP expression ($n = 15$ for MG EM, $n = 15$ for MG DM, $n = 40$ for CNF), F) CYP3A4 expression ($n = 15$ for MG EM, $n = 15$ for MG DM, $n = 40$ for CNF), G) HNF4a expression ($n = 15$ for MG EM, $n = 15$ for MG DM, $n = 41$ for CNF), H) LGR5 expression ($n = 12$ for MG EM, $n = 12$ for MG DM, $n = 33$ for CNF), I) MRP2 expression ($n = 15$ for MG EM, $n = 15$ for MG DM, $n = 42$ for CNF), J) SULT expression ($n = 12$ for MG EM, $n = 13$ for MG DM, $n = 29$ for CNF), K) UGT expression ($n = 15$ for MG EM, $n = 14$ for MG DM, $n = 35$ for CNF). All data depicted as mean ± SD (*$p < 0.05$, **$p < 0.01$, ***$p < 0.001$, ****$p < 0.0001$, ns: not significant), ANOVA with Tukey's post-hoc test.

and polarization marker.[25] It is clearly visible that MRP2 stains more positive in the apical membrane of the organoids in CNF hydrogel and accumulates more toward the luminal side of the organoid (Figure 6I), whereas the staining is more positive toward the basal part of the organoid for MG (Figure 6H). The staining in EM condition is negative. Similarly, the tight junction protein ZO1 should be located toward the end of the

lateral membrane in proximity to the bile cuniculi, indicating the polarity of hepatocytes.[25] It is observed in Figure 6L that the staining for ZO1 in CNF hydrogel is clearly located along the plasma membrane with a preference for the basal side of the organoid, while the staining is less specific for both MG conditions (Figure 6J,K). Accumulation of glycogen in the differentiated organoids is observed in both CNF hydrogel and
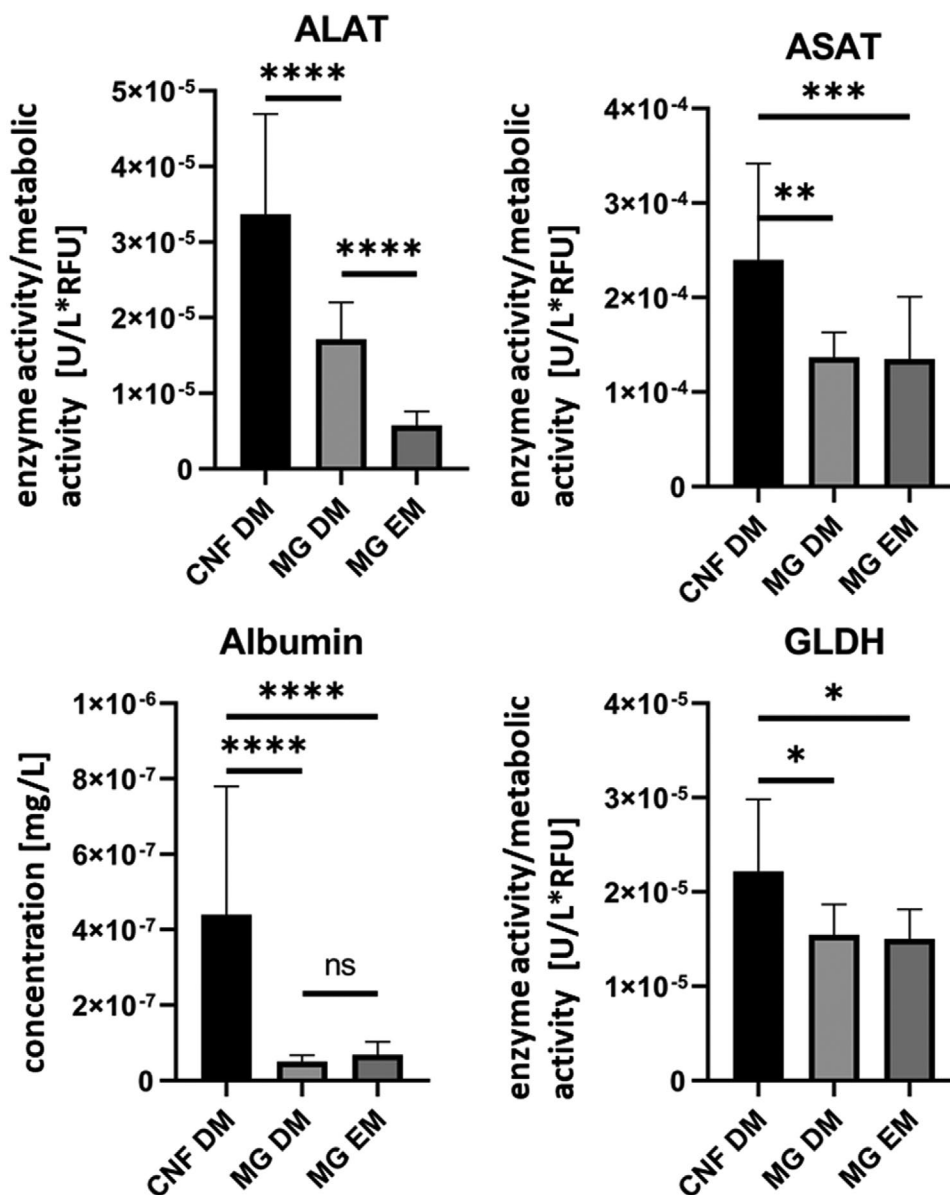
Figure 5. Functional read-out in relative enzyme activity and albumin concentration corrected to the metabolic activity of hepatocyte-like cells lysed after 7 days of differentiation in cellulose nanofibril (CNF) hydrogel (data averaged over all concentrations) and Matrigel (MG) in differentiation medium (DM) (CNF DM ($n = 16$ for Albumin and GLDH, $n = 24$ for ALAT and ASAT), MG DM ($n = 6$ for Albumin and GLDH, $n = 9$ for ALAT and ASAT)) as well as in MG in expansion medium (EM) (MG EM ($n = 6$ for Albumin and GLDH, $n = 9$ for ALAT and ASAT)) as comparison. Data are averaged over all donors, all data depicted as mean ± SD (*$p < 0.05$, **$p < 0.01$, ***$p < 0.001$, ****$p < 0.1$, ns: not significant), ANOVA with Tukey's post-hoc test.

MG (Figure 6N,O) at higher levels compared to EM conditions (Figure 6M).

3. Discussion

In this study, we have shown that CNF hydrogels are a viable alternative for MG and improve the hepatic differentiation of organoids. In the current configuration, the CNF hydrogel does not sustain organoid proliferation (data not shown) but does induce hepatic maturation. The positive attributes of CNF hydrogel and its potential for organoid differentiation are discussed below.

3.1. CNF Hydrogel Characterization

The relatively high resistance of CNF hydrogel to strain is an indicator for constant remodeling of the nanofibril network,[26] even in an atomic force microscopy image of a very low CNF concentration (0.005% w/v) it has been shown that the nanofibrils are very densely packed and prevent the cells from working around the fibers.[18] The self-healing character of the gel was demonstrated by the alternating strain experiment. The reversible switch of dominance between G' and G'' at high strains show that the CNF hydrogel network broke down and flowed like a viscous solution but recovered completely
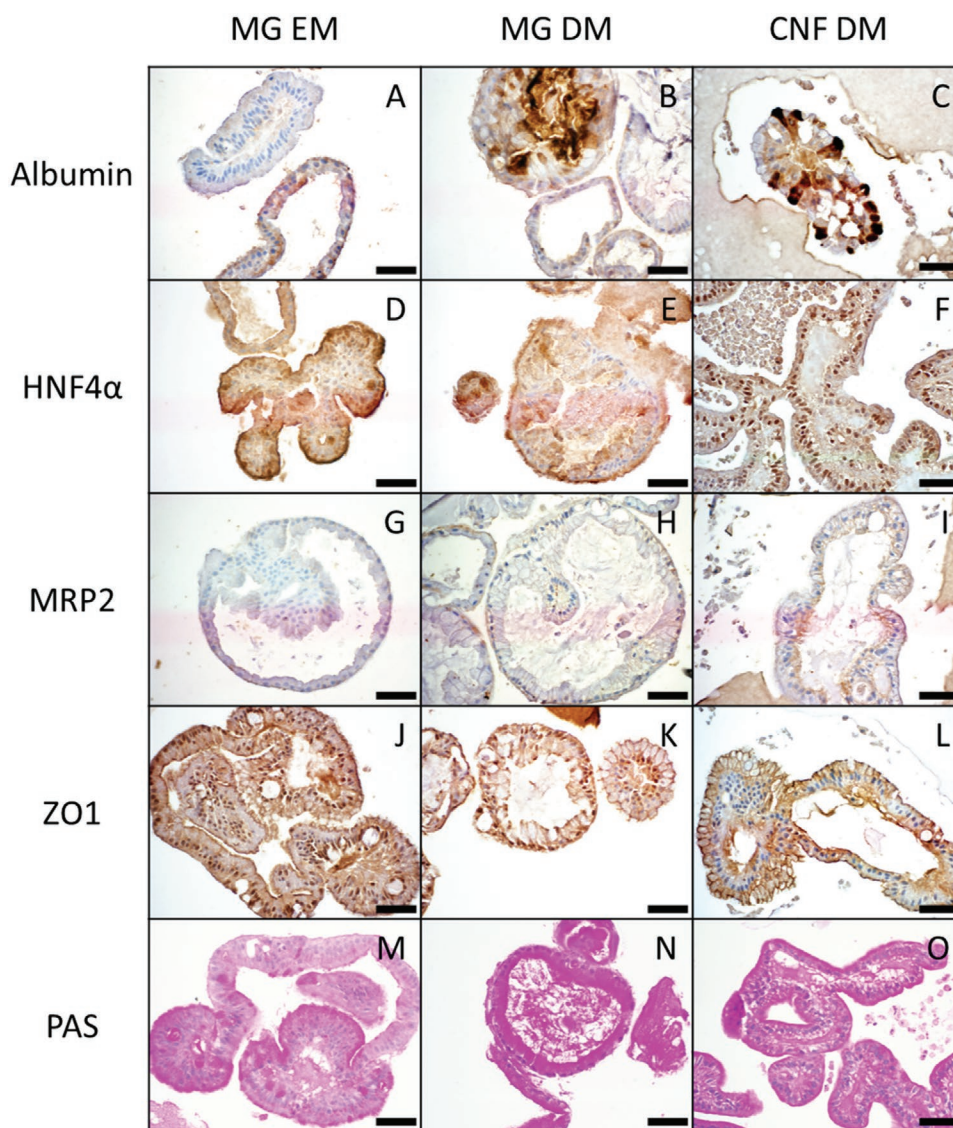
Figure 6. Representative immunohistochemical and periodic acid–Schiff (PAS) stainings of human liver organoids cultured in Matrigel (MG) or cellulose nanofibril (CNF), respectively. A) Albumin staining, MG EM, donor h2; B) Albumin staining, MG DM, donor h5; C) Albumin staining, CNF 0.2, donor h5; D) HNF4a staining, MG EM, donor h2; E) HNF4a staining, MG DM, donor h2; F) HNF4a staining, CNF 0.2, donor h2; G) MRP2 staining, MG EM, donor h2; H) MRP2 staining, MG DM, donor h2, I) MRP2 staining, CNF 0.6, donor h2; J) ZO1 staining, MG EM, donor h5; K) ZO1 staining, MG DM, donor h5; L) ZO1 staining, CNF 0.6, donor h5; M) PAS staining, MG EM, donor h5; N) PAS staining, MG DM, donor h2; O) PAS staining, MG EM, donor h2. Scale bar: 50 µm.

without any loss of its properties, which shows that there was no destruction on the molecular level.[26] The low gradient of G' and G'' in the frequency sweep demonstrated that the gel had a strong internal network and is quite structured.[26] Compared to CNF hydrogel, MG exhibits similar behavior at lower frequencies but the crossover point of G' and G'' is already below 100 rad s^{-1}. [27] For CNF, the storage modulus G' decreased linearly up to 13% strain, which is similar compared to MG, but in contrast to the CNF hydrogel, MG has a very low viscous response, which is demonstrated by the unmeasurable loss modulus G''.[27] In addition, MG does not possess the capability to restore its structure after release like CNF hydrogel. The lack of self-healing properties are a major reason for the absence

of successful permanently cross-linked hydrogels in clinical settings.[28] Therefore, the CNF hydrogel has an advantage in tissue engineering and regenerative medicine due to its unique properties, as it is injectable due to its shear-thinning character and self-healing after breaking.

The observed swelling of CNF hydrogel in demineralized water is caused by the Higgs–Donnan effect,[29] where the deprotonation of the C6 carboxyl group of the hydrogel results in water entering into the gel to equalize the difference in osmotic pressure. Therefore, the gel will not stop swelling until it is completely dissolved in water. Deprotonation is not possible in PBS, therefore, no negative charges lead to swelling of the gel. This means that CNF hydrogel is stable in

**ADVANCED
SCIENCE NEWS**
www.advancedsciencenews.com

**ADVANCED
HEALTHCARE
MATERIALS**
www.advhealthmat.de

salt-containing solutions as medium used for organoid cultures but can be swollen and disintegrated into demineralized water.

3.2. Human Liver Organoid Performance

Expansion of human liver organoids in CNF hydrogel is not successful, as metabolic activity in the CNF hydrogel does not significantly increase over time as opposed to MG. This might be caused by the characteristics of the hydrogel, which through its mechanical properties, and potentially mismatch in degradation rate, may limit the organoids in proliferation. It has been shown that organoid formation and expansion occurs in a narrow mechanical window; stiffer gels support expansion (1.3 kPa for intestinal organoids), whereas differentiation requires softer gels (0.2 kPa).[30] However, little is known about how the mesh size and degradation rate of the hydrogel affects these processes, even though they are highly coupled to the mechanical properties. Generally, cells sense the bulk scaffold elasticity, while in viscoelastic materials they can further mechanically remodel their surrounding depending on the relaxation rate and cell type.[31] In future investigations, the mechanical properties of the CNF hydrogel could be adapted to suit the application of organoid expansion, and softened over time through controlled enzymatic degradation. Additionally, ECM components proven to be advantageous for organoid growth, such as laminin-111, collagen IV, and fibronectin, could be incorporated.[32]

Morphological appearance and metabolic activity results of the human liver organoids in MG in EM and DM conditions are consistent with previously shown results.[9] The morphology of the organoids in CNF hydrogel appear darker, not as round and with a less even surface as compared MG cultures. This is due to an inversed polarity of the cells where the apical side of the organoid is oriented outwards and presents this more irregular appearance, as has been previously shown for intestinal organoids.[33] This change in polarity was corroborated with immunocytology showing polarity-specific proteins and is due to the lack of ECM proteins regulating the polarity in the CNF hydrogel that are present in MG.[33] Where the ECM components are in direct contact with the cells, it creates the basolateral membrane. Especially laminins are believed to cause this effect which lead to a cascade of integrin signaling and establishes polarity.[34]

As opposed to MG, organoids in CNF hydrogel presented a decrease in metabolic activity within the first 4 days, which was most likely caused by cell death due to the different exposure of organoids during initial handling. Because the CNF hydrogel coagulates and loses its self-healing characteristic when mixed with salt-containing solutions, the organoids extracted from the MG, where they were expanded in, were mixed with the CNF hydrogel in the presence of demineralized water, while media was directly added after plating of the hydrogel. The loss of its self-healing characteristics is hypothesized to be caused by protonation of the CNF hydrogel's carboxyl groups by sodium cations. Because of the positively charged sodium cations, the previously negatively charged carboxyl groups lose their repulsive forces, which are required for the materials self-healing character through ionic interactions[17] and therefore CNFs

agglomerates. Thus, the organoids placed in the CNF hydrogel needed to adjust to the new environmental conditions, which resulted in a reduced viability at the beginning of differentiation. On the other hand, metabolic activity levels prove that the cells stabilized and stayed viable over the remaining culture period. After an initial acceptable reduction of 23% in metabolic activity, cells regained their stability once culture medium was added and diffused into the gel, delivering the necessary nutrients for cell survival and function. In a previous report, a similar effect was observed, where fibroblasts spheroids inside CNF hydrogel first demonstrated a dead outer cell layer upon inclusion into the hydrogel to then recover viability in this area after a culture period of 2 weeks.[24] This effect could in the future be alleviated by introducing other groups, which cannot be protonated, onto the surface of the CNFs instead of the carboxyl groups. In addition, incorporation of moieties that stimulate cell activity and proliferation, as shown in other hydrogels,[35] could improve the overall functionality of the hepatocyte-like organoids.

Apart from the surrounding medium conditions that influence the liver organoid cells, another factor is the stiffness of the gel. As MG and 0.6% (w/v) CNF hydrogel are soft hydrogels according to their Young's moduli ($\approx$255 Pa for CNF hydrogel and +440 Pa for MG [36]), there is no great difference on the macroscale. It is known that the ECM close to hepatocytes is soft ($E \approx 1.5$ kPa)[37] and that soft surfaces promote hepatic stem cells to differentiate into hepatocytes.[38] On the other hand, soft matrices have also proven to be beneficial for intestinal organoid differentiation.[30] Importantly, despite the low Young's modulus, CNF hydrogel is composed of very stiff nanofibrils ($E = 138$ GPa),[18,19] providing mechanical cues on the nanoscale that can influence cell differentiation and performance.[37] The hepatic organoids in CNF hydrogel appeared much darker and differently shaped compared to MG, which could be due to collapse and folding caused by mechanical forces and/or the lack of growth factors, laminin, and adhesion sites in the CNF hydrogel. However, this difference in appearance did not have a negative effect on the performance of the differentiated organoids. Remarkably, liver organoids were still able to form in the CNF hydrogel and fuse together into larger constructs, although the gel is not degradable without the addition of the enzyme cellulase.[14,22,23] This indicates that the environment can adapt to the organoid structures and is beneficial for the cells.

The functionality of the hepatocyte-like cells in CNF hydrogel was on average higher when the different read-outs were compared. The organoids in the CNF hydrogel were metabolically active and produced higher levels of enzymes (ALAT, ASAT, GLDH, albumin) compared to MG. Overall, differentiation in CNF hydrogels seemed to have occurred at a higher level compared to MG, which is also indicated by the significantly higher levels of albumin production compared to both MG DM and MG EM. However, this observation is not confirmed by the gene expression analysis, which shows that albumin was expressed at similar levels in either hydrogel in DM condition, but significantly higher than in the EM condition. In addition, immunostaining presented a similar expression of albumin, albeit oppositely located in the organoid. Even though some conflicting results may be caused by the large variability in data

1901658 (8 of 12)

**ADVANCED
SCIENCE NEWS**
www.advancedsciencenews.com

**ADVANCED
HEALTHCARE
MATERIALS**
www.advhealthmat.de

in the case of albumin enzyme activity among all functional read-outs, it can still be concluded that all analysis methods reveal that albumin production is at least as high in the CNF hydrogel as in MG. In contrast, the differentiation marker LGR5 did show higher expression levels in CNF hydrogel compared to MG, which indicates that more stem cells were still present in CNF after differentiation. On the other hand, even though the marker for hepatocyte fate, HNF4a, did not show a significant difference in gene expression, the immunostaining demonstrated more specific nuclear staining in the case of CNF hydrogel as opposed to MG, indicating that indeed the cells developed into functional hepatocytes. This finding is emphasized by the expression levels of the enzymes that are involved in the metabolism of xenobiotics (phase I to III), which show that the CNF hydrogel performed at least equally as well as the gold standard of MG and was even superior in two cases (CYP3A4 and SULT). In all tested genes except for CYP1A2, which did not display any differences, expression levels showed successful differentiation, as they were consistently higher than levels in organoids remaining in EM. Results are comparable to other organoid studies in MG and poly(ethylene glycol) hydrogels,[9,35,39] as well as with cell lines (HepaRG progenitor cells) in nanofibrillar cellulose and hyaluronan-gelatin (HG) hydrogels.[8]

Although the expression of the hepatic markers was higher in the CNF conditions compared to MG, the overall expression of these genes in native hepatocytes and liver samples were still higher. This shows that the liver organoids still did not fully reach the same maturity. It is known that several other factors in the microenvironment are needed to improve this hepatic maturation, including co-culture, smaller microgels produced with microfluidics, amongst others.[40] Interestingly, both the polarization markers MRP2 and ZO1, which are located at the apical membrane of a native hepatocyte and at the apical membrane or in close proximity thereof, respectively,[25,41] showed a different localization in organoids cultured in CNF hydrogel compared to MG. Polarization of cells is induced by the ECM in livers or by ECM mimicking materials in vitro and is very important for the function of the cells.[3] The needed apicobasal polarity can be found in both CNF hydrogel and MG, however, it was more pronounced in CNF but polarity was inversed. In the CNF hydrogel, the basal membrane of the hepatocytes was facing away from the lumen, which presents advantages for toxicity and drug uptake testing, because the compounds would not have to be included inside the organoids but can be administered with the medium from the outside. The MRP2 and ZO1 staining further indicate the formation of bile canaliculi-like structures, another hallmark for the structure of liver tissue.

An extensive review on hydrogels for liver tissue engineering has been published recently, naming many advantages and disadvantages of multiple natural and synthetic hydrogels with respect to the specific demands for liver tissue engineering.[3] Biocompatible CNF hydrogel specifically fulfils some of these requirements as it has the ability to culture autologous cell sources, as also proven in this study.[6,8,12,21] Furthermore, previous studies have shown that there is a potential for vascular tissue engineering in CNF material[14,20,42] and the chemistry allows for the addition of bioactive functional groups on to the fiber surface. As previously mentioned, the CNF hydrogel has

a defined chemistry from only plant origin, which in principle would enable FDA approval[3] and compliance with GMP conditions, opening up the possibility for clinical translation.[43] Due to its mechanical properties in the required range of 0.2–1 kPa[3] and its shear-thinning characteristic, CNF hydrogel is suitable for bioprinting and through the addition of cellulase enzymes, it is also degradable.[12,22,24]

4. Conclusion

In conclusion, this study shows that the differentiation of liver organoids into functional hepatocyte-like cells is at least as successful in CNF hydrogel compared to MG and sometimes superior The TEMPO-oxidized CNF hydrogel showed advantages with regard to the expression of hepatic genes, overall hepatocyte function, and organoid polarization. In combination with the natural biocompatibility, the mechanical properties of CNF hydrogels, such as the rapid self-healing and shear-thinning behavior, prove to provide a supportive environment for the differentiation of liver organoids and offer to be a good alternative to MG in tissue engineering and regenerative medicine. Further improvements might be possible through the addition of the degrading cellulase enzyme,[24] adding other bioactive moieties to the nanofibrils, producing smaller CNF microgels, or by further tuning of the elastic modulus of the hydrogel.[17]

5. Experimental Section

CNF Hydrogel: The CNF hydrogel was produced with the TEMPO method, where paper pulp (Papiertechnische Stiftung, Heidenau, Germany) was oxidized, then dispersed in water and homogenized under high pressure.[18,44,45] Sterility was achieved by autoclaving the gel at 121 °C for 20 min. The stock concentration of cellulose (CNF) after this procedure was 0.6% (w/v) (CNF 0.6) at a pH of 6. The 0.6% (w/v) CNF hydrogel was diluted with sterile demineralized water to 0.4% (w/v) (CNF 0.4) and 0.2% (w/v) (CNF 0.2).

Organoid Expansion and Differentiation: Human liver organoid cultures were generated from three independent, anonymized adult organ donors. Tissue samples (<0.5 cm³) of donor liver biopsies collected during liver transplantation at the Erasmus Medical Center Rotterdam were routinely taken to test for any liver pathology. Use of these tissues for research purposes was approved by the Medical Ethical Council of the Erasmus MC and informed consent was given by recipients (MEC-2014-060). Biopsies were stored in ice cold organ preservation fluid (University of Wisconsin Solution, Bridge of Life Ltd, London, UK) for transportation and processed for organoid-initiation as described previously.[8] In short, cells were cultured in MG (Corning, New York, NY, USA) droplets in 24-well plates in EM for up to 13 passages. EM consisted of Advanced DMEM/F12 supplemented with 1% (v/v) penicillin-streptomycin (ThermoFisher, Waltham, MA, USA), 1% (v/v) GlutaMax (ThermoFisher), 10 mM HEPES (ThermoFisher), 2% (v/v) B27 supplement without vitamin A (Invitrogen, Carlsbad, CA, USA), 1% N2 supplement (Invitrogen), 10×10^{-3} M nicotinamide (Sigma-Aldrich, Zwijndrecht, the Netherlands), 1.25×10^{-3} M *N*-acetylcysteine (Sigma-Aldrich), 10% (v/v) R-spondin-1 conditioned medium (the Rspo1-Fc-expressing cell line was a kind gift from Calvin J. Kuo), 10×10^{-6} M forskolin (Sigma-Aldrich), 5×10^{-6} M A83-01 (Tocris Bioscience, Bristol, UK), 50 ng mL^{-1} EGF (Invitrogen), 25 ng mL^{-1} HGF (Peprotech, London, UK), 0.1 mg mL^{-1} FGF10 (Peprotech), 10×10^{-9} M recombinant human (Leu15)-gastrin I (Sigma-Aldrich), and 0.1 mg mL^{-1} Noggin (Peprotech).

To assess the possibility to expand liver organoids in CNF hydrogel, organoids cultured in MG (Corning) were reseeded into either 50 μL

fresh MG, CNF 0.4 or CNF 0.6 ($n = 3$ for each condition) and cultured with 500 µL EM medium for 7 days with medium changes on days 2 and 4.

For the differentiation experiments, EM was supplemented with 25 ng mL^{-1} BMP-7 (Peprotech) 4 days prior to organoid transfer and the start of differentiation. At the start of differentiation, the organoids were reseeded into 50 µL MG or CNF hydrogels (CNF 0.2, CNF 0.4, CNF 0.6) and DM was added. DM consisted of EM without R-spondin-1 and nicotinamide but with the addition of 25 ng mL^{-1} BMP7 (Peprotech), 10×10^{-6} M DAPT (γ-secretase inhibitor, Selleckchem, Houston, TX, USA), 100 ng mL^{-1} FGF19 (R&D Systems, Minneapolis, MN, USA), and 30×10^{-6} M dexamethasone (Sigma-Aldrich). Media was refreshed on days 4 and 6 until the culture was terminated on day 7. In the case of MG, EM was added as a control.

Analyses—Hydrogel Characterization: Rheological tests to characterize the material ($n = 1$) were performed on the stock concentration of 0.6% (w/v) CNF hydrogel with a 1HR-3 DHR-3 rheometer in combination with a SST ST 20 mm 2° smart-sweep cone plate and analyzed with Texas Instrument TRIOS software (Texas Instruments, Dallas, TX, USA). The protocol for characterization of a hydrogel was applied as described by Zuidema et al.[27] and adopted according to Rowland et al.[26] For all measurements, 400 µL of CNF hydrogel was used, the gap between plates was set to 0.5 mm, and temperature was constant at 20 °C. The gel was soaked for 60 s to allow the gels to swell after compression and equilibrate to the temperature. Dynamic oscillatory amplitude sweep measurements were taken at 1 rad s^{-1} and oscillatory frequency sweep measurements were conducted at 0.5% oscillating strain. For altering strain experiments, the strain was altered between 1% and 500% in periods of 30 s and flow sweeps were conducted with 5 s equilibration time and 30 s averaging time. The Young's modulus (E) was calculated by determining the plateau value of the frequency sweep (G'_e) and with an assumed Poisson's ratio (ν) of 0.5 of incompressible materials according to Equation (1):

$$E = 2 \times G'_e (1 + \nu) \tag{1}$$

Swelling of the prepared gel was measured by submerging 0.5 of the 0.6% (w/v) CNF hydrogel in 2 mL demineralized water and 1× PBS for 30 min, 1 h, and 4 h and the liquid is renewed after 2 min, 20 min, and then every hour ($n = 3$). For each timepoint, the swelling ratio is calculated by measuring the wet weight of the swollen gels with the cellulose concentrations before and after swelling.

Analyses—Morphology: The morphology of the organoids was followed over time for all conditions and brightfield images were taken at days 1 and 7 after the start of differentiation with an Olympus Color CCD microscope (CKX41, Tokyo, Japan), Leica DFC425C camera, and accompanying Leica-suite software (Wetzlar, Germany), and postprocessed with Image-J software (NIH, Madison, WI, USA).

Analyses—Metabolic Activity: Metabolic activity of the organoids in all conditions was measured on days 1, 4, 6, and 7 (days 2, 4, and 7 for the expansion experiment) with the Alamar Blue assay (Invitrogen) with $n = 3$ per condition. The Alamar Blue solution was diluted to 10% (v/v) with Advanced DMEM/F12 medium (Gibco) and incubated in three wells for each hydrogel condition and donor, and wells with gel but without organoids ($n = 3$ per condition) for 2 h. Fluorescence was measured at 540–590 nm with a DxC-600 Beckman plate reader (Beckman Coulter, Brea, CA, USA) and the levels of the wells without organoids were subtracted from the read-outs for background correction. All values were compared to day 1, which was set to 100% of metabolic activity.

Analyses—Gene Expression: Gene expression analysis on all conditions (MG, CNF 0.2, CNF 0.4, CNF 0.6) and respective medium condition (DM, EM) were used to assess the differentiation status of the organoids ($n = 6$ per condition). The samples were lysed with 350 µL RLT buffer (Qiagen, Hilden, Germany) containing 1% (v/v) 2-Mercaptoethanol (Sigma-Aldrich). Isolation of mRNA was done according to the manufacturer's instructions with a RNeasy micro-kit (Qiagen) and the total mRNA was measured with a NanoDrop ND-1000 spectrophotometer (ThermoFisher Scientific, Breda, The Netherlands)

Table 1. Primers used for quantitative PCR (qPCR) analysis.

Gene	Forward	Reverse
RPL19	ATGAGTATGCTCAGGCTTCAG	GATCAGCCCATCTTTGATGAG
GAPDH	TGCACCACCAACTGCTTAGC	GGCATGGACTGTGGTCATGAG
LGR5	GCAGTGTTCACCTTCCC	GGTCCACACCCAATTCTG
KRT19	CTTCCGAACCAAGTTTGAGAC	AGCGTACTGATTTCCTCCTC
ALB	GTTCGTTACACCAAGAAAGTACC	GACCACGGATAGATAGTCTTCTG
HNF4A	GTACTCCTGCAGATTTAGCC	CTGTCCTCATAGCTTGACCT
CYP3A4	TGATGGTCAACAGCCTGTGCTGG	CCACTGGACCAAAAGGCCTCCG
CYP1A2	CCCAGAATGCCCTCAACA	CCACTGACACCACCACCTGAT
CYP2D6	GAGGTGCTGAATGCTGTC	AGGTCATCCTGTGCTCAG
CYP2C19	GGGACAGAGACAACAAGCA	CCTGGACTTTAGCTGTGACC
UGT	AATACTCGGCTGTATGATTGG	CATAGATCCCATTCATTCCACC
SULT	TTCCTTGAGTTCAAAGCCC	TGTCTTCAGGAGTCGTGG
MRP2	GCCAACTTGTGGCTGTGATAGG	ATCCAGGACTGCTGTGGGACAT
BSEP	TTGAGACAATAGACAGGAAACC	TCTGGAAGGATAATGGAAGGT

at 260–280 nm. For the synthesis of complementary DNA (cDNA) from 500 ng mRNA, the manufacturer's protocol for the used iScript cDNA Synthesis Kit (Bio-Rad, Hercules, CA, USA) was applied. Quantitative PCR (qPCR) was performed using a Bio-Rad CFX384 Real-Time PCR Detection System (Bio-Rad) with 10 ng cDNA per reaction and iQ SYBR Green Supermix (Bio-Rad). Primers are listed in **Table 1**. Data were analyzed with Bio-Rad CFX manager software (CFX Maestro, Bio-Rad), relative gene expression was calculated according to the $2^{-\Delta CT}$ formula and normalized to the reference genes GAPDH and RPL19. As reference, samples from hepatocytes pooled from 10 donors (mixed gender, LiverPool Cryoplateable Hepatocytes, BioreclamationIVT, Brussels, Belgium) and a whole liver sample from one donor were added to the analysis.

Analyses—Hepatic Function: To measure the enzyme activity, the same samples used for metabolic activity analysis ($n = 3$ per condition) were lysed with Milli-Q water (Merck, Millipore, Burlington, MA, USA). Subsequently, ALAT, ASAT, Albumin, GLDH, as well as total protein, were measured with the clinical chemistry analyzer Beckman AU680 (Beckman Coulter) using standard protocols. Finally, albumin values were corrected for total protein levels and all enzyme values were divided by the metabolic activity values to correct for the number of viable cells.

Analyses—Histology: Hydrogel samples from each condition ($n = 2$ per condition) were fixed with 4% paraformaldehyde and embedded in paraffin. For stainings, 5 µm sections were cut and sections were deparaffinized and rehydrated.

For immunohistochemistry, the slides were blocked in 10% (v/v) normal goat serum (Bio-Rad), after antigens were retrieved. Antigen retrieval for albumin and HNF4a staining was achieved with a 10 mM Tris−1 mM EDTA solution (both Sigma-Aldrich) with 0.5% Tween 20 (Merck KGaA, Darmstadt, Germany) at pH 9.0 for 30 min at 98 °C. For MRP2 antigen retrieval was performed with a 10 mM citrate buffer (Merck) at pH 6 for 30 min at 98 °C and ZO1 antigen retrieval was performed with 0.4% (w/v) pepsin (Dako, Santa Clara, CA, USA) in 0.2 N HCl (Merck) for 20 min at 37 °C. The primary antibody for albumin (A6684, Sigma-Aldrich), was incubated in a 1:1000 dilution; HNF4a (sc8987, Santa Cruz, Dallas, TX, USA) in a 1:300 dilution; MRP2 (Mon9027, Monosan, Uden, the Netherlands) in a 1:75 dilution; and ZO1 (40-2300, Invitrogen) in a 1:250 dilution, all incubations were performed overnight at 4 °C. The wash buffer for albumin, HNF4a, MRP2, and ZO1 was PBS + 0.1% (v/v) Tween 20. Envisioning of the antibodies was achieved with goat-anti-mouse/rabbit HRP (ImmunoLogic, Amsterdam, the Netherlands) and DAB/metal (ImmunoLogic) concentrate. As a counterstain hematoxylin (Dako, Glostrup, Denmark) was applied and slides were mounted with Vectamount (Vector Laboratories,

Peterborough, UK) after dehydration. Images were taken on the Olympus BX60 microscope (Olympus, Leiderdorp, the Netherlands) and processed with Image-J software (NIH, Madison, WI, USA).

PAS Staining: The PAS staining was performed by the Veterinary Pathology Diagnostics Centre in Utrecht according to the standardized procedures.

Statistical Analysis: Extreme outliers with values more than three times the interquartile range were identified for each outcome parameter and excluded from further analysis using SPSS Statistics 25 (IBM, Armonk, NY, USA). Statistical analysis for all data was performed with Graphpad Prism 8 (San Diego, CA, USA).

For the metabolic activity studies with averaged CNF hydrogel concentrations, a two-way ANOVA analysis was performed followed by a Tukey post-hoc test. For the metabolic activity study comparing different CNF hydrogel conditions, multiple *t*-tests using the Holm–Sidak method were executed. After careful investigation of all data, no significant differences between the different CNF hydrogel concentrations were found (see Figures S2, S3, S4, Supporting Information). Therefore, data for each read-out of all CNF hydrogel concentrations were averaged in further analysis. Data of transaminase activity and gene expression averaged over CNF hydrogel concentrations were log-transformed and then a one-way ANOVA was performed with Tukey's post-hoc test. Data of transaminase activity and gene expression comparing different CNF hydrogel concentration were log-transformed and then a mixed-effects analysis was performed to account for missing values followed by Tukey's post-hoc test. All transformed data were back transformed for reporting. All analyzed data were normally distributed and had equal variances as tested by examining the normal Q–Q plot of residuals and the scatter plots of residuals over predicted values, respectively. Differences were considered statistically significant for $p < 0.05$, and *p*-values were depicted in the figures, where asterisks represented the statistical significance (*$p < 0.05$, **$p < 0.01$ ***$p < 0.001$, ****$p < 0.0001$, ns: not significant). Furthermore, *n* refers to the sample size for each statistical analysis. Data were presented as a box diagram with median and 25th and 75th percentiles and whiskers from min to max for metabolic activity (DM conditions) data and bar graphs with mean and standard deviation for all other data sets.

Supporting Information

Supporting Information is available from the Wiley Online Library or from the author.

Acknowledgements

Conflict of Interest

The authors declare no conflict of interest.

Keywords

[1] S. L. Murphy, J. Xu, K. D. Kochanek, S. C. Curtin, E. Arias, *Natl. Vital Stat. Rep.* **2017**, *66*, 1.

[2] C. Rudge, R. Matesanz, F. L. Delmonico, J. Chapman, *Br. J. Anaesth.* **2012**, *108*, i48.

[3] S. Ye, J. W. B. Boeter, L. C. Penning, B. Spee, K. Schneeberger, *Bioengineering* **2019**, *6*, 59.

[4] A. Ananthanarayanan, B. C. Narmada, X. Mo, M. McMillian, H. Yu, *Trends Biotechnol.* **2011**, *29*, 110.

[5] M. D. Leise, J. J. Poterucha, J. A. Talwalkar, *Mayo Clin. Proc.* **2014**, *89*, 95.

[6] M. Bhattacharya, M. M. Malinen, P. Lauren, Y. R. Lou, S. W. Kuisma, L. Kanninen, M. Lille, A. Corlu, C. Guguen-Guillouzo, O. Ikkala, A. Laukkanen, A. Urtti, M. Yliperttula, *J. Controlled Release* **2012**, *164*, 291.

[7] A. V. Janorkar, L. M. Harris, B. S. Murphey, B. L. Sowell, *Biotechnol. Bioeng.* **2011**, *108*, 1171.

[8] M. M. Malinen, L. K. Kanninen, A. Corlu, H. M. Isoniemi, Y.-R. Lou, M. L. Yliperttula, A. O. Urtti, *Biomaterials* **2014**, *35*, 5110.

[9] M. Huch, H. Gehart, R. Van Boxtel, K. Hamer, F. Blokzijl, M. M. A. Verstegen, E. Ellis, M. Van Wenum, S. A. Fuchs, J. De Ligt, M. de Wetering, N. Sasaki, S. J. Boers, H. Kemperman, J. de Jonge, J. N.M. Ijzermans, E. E. S. Nieuwenhuis, R. Hoekstra, S. Strom, R. R. G. Vries, L. J. W. van der Laan, E. Cuppen, H. Clevers, *Cell* **2015**, *160*, 299.

[10] T. H. Booij, L. S. Price, E. H. J. Danen, *SLAS Discov.* **2019**, *24*, 615.

[11] K. Schneeberger, B. Spee, P. Costa, N. Sachs, H. Clevers, J. Malda, *Biofabrication* **2017**, *9*, 013001.

[12] Y.-R. Lou, L. Kanninen, T. Kuisma, J. Niklander, L. A. Noon, D. Burks, A. Urtti, M. Yliperttula, *Stem Cells Dev.* **2014**, *23*, 380.

[13] C. S. Hughes, L. M. Postovit, G. A. Lajoie, *Proteomics* **2010**, *10*, 1886.

[14] L. Bačáková, K. Novotná, M. Pařzek, *Physiol. Res.* **2014**, *63*, S29.

[15] T. Saito, T. Uematsu, S. Kimura, T. Enomae, A. Isogai, *Soft Matter* **2011**, *7*, 8804.

[16] J.-L. Putaux, A. Isogai, T. Saito, Y. Nishiyama, M. Vignon, *Biomacromolecules* **2006**, *7*, 1687.

[17] K. Syverud, S. R. Pettersen, K. Draget, G. Chinga-Carrasco, *Cellulose* **2015**, *22*, 473.

[18] J. G. Torres-Rendon, T. Femmer, L. De Laporte, T. Tigges, K. Rahimi, F. Gremse, S. Zafarnia, W. Lederle, S. Ifuku, M. Wessling, J. G. Hardy, A. Walther, *Adv. Mater.* **2015**, *27*, 2989.

[19] J. G. Torres-Rendon, M. Köpf, D. Gehlen, A. Blaeser, H. Fischer, L. De Laporte, A. Walther, *Biomacromolecules* **2016**, *17*, 905.

[20] P. Pooyan, R. Tannenbaum, H. Garmestani, *J. Mech. Behav. Biomed. Mater.* **2012**, *7*, 50.

[21] P. Pooyan, I. T. Kim, K. I. Jacob, R. Tannenbaum, H. Garmestani, *Polymer* **2013**, *54*, 2105.

[22] Y. Hu, J. M. Catchmark, *J. Biomed. Mater. Res., Part B* **2011**, *97B*, 114.

[23] A. Sannino, C. Demitri, M. Madaghiele, *Materials* **2009**, *2*, 353.

[24] M. Krueger, B. Spee, A. Walther, L. De Laporte, L. M. Kock, *ASME J. Eng. Sci. Med. Diagn. Ther.* **2019**, *2*, 041001.

[25] T. Mitaka, H. Ooe, *Drug Metab. Rev.* **2010**, *42*, 472.

[26] M. J. Rowland, M. Atgie, D. Hoogland, O. A. Scherman, *Biomacromolecules* **2015**, *16*, 2436.

[27] J. M. Zuidema, C. J. Rivet, R. J. Gilbert, F. A. Morrison, *J. Biomed. Mater. Res., Part B* **2014**, *102*, 1063.

[28] L. Saunders, P. X. Ma, *Macromol. Biosci.* **2019**, *19*, e1800313.

[29] J. Grignon, A. M. Scallan, *J. Appl. Polym. Sci.* **1980**, *25*, 2829.

[30] N. Gjorevski, N. Sachs, A. Manfrin, S. Giger, M. E. Bragina, P. Ordóñez-Morán, H. Clevers, M. P. Lutolf, *Nature* **2016**, *539*, 560.

[31] L. C. Bahlmann, A. Fokina, M. S. Shoichet, *MRS Commun.* **2017**, *7*, 472.

[32] G. Sorrentino, S. Rezakhani, E. Yildiz, S. Nuciforo, M. H. Heim, M. P. Lutolf, K. Schoonjans, *bioRxiv* **2019**, https://doi.org/10.1101/810275.

[33] J. Y. Co, M. Margalef-Català, X. Li, A. T. Mah, C. J. Kuo, D. M. Monack, M. R. Amieva, *Cell Rep.* **2019**, *26*, 2509.

[34] J. L. Lee, C. H. Streuli, *J. Cell Sci.* **2014**, *127*, 3217.

[35] B. J. Klotz, L. A. Oosterhoff, L. Utomo, K. S. Lim, Q. Vallmajo-martin, H. Clevers, T. B. F. Woodfield, A. J. W. P. Rosenberg, J. Malda, M. Ehrbar, B. Spee, D. Gawlitta, *Adv. Healthcare Mater.* **2019**, *8*, 1900979.

[36] S. S. Soofia, J. A. Lasta, S. J. Liliensieka, P. F. Nealeyb, C. J. Murphy, *J. Struct. Biol.* **2009**, *167*, 216.

[37] G. C. Reilly, A. J. Engler, *J. Biomech.* **2010**, *43*, 55.

[38] E. Jain, A. Damania, A. Kumar, *Hepatol. Int.* **2014**, *8*, 185.

[39] H. S. Kruitwagen, L. A. Oosterhoff, I. G. W. H. Vernooij, I. M. Schrall, M. E. van Wolferen, F. Bannink, C. Roesch, L. van Uden, M. R. Molenaar, J. B. Helms, G. C. M. Grinwis, M. M. A. Verstegen, L. J. W. van der Laan, M. Huch, N. Geijsen, R. G. Vries, H. Clevers, J. Rothuizen, B. A. Schotanus, L. C. Penning, B. Spee, *Stem Cell Rep.* **2017**, *8*, 822.

[40] C. Chen, A. Soto-Gutierrez, P. M. Baptista, B. Spee, *Gastroenterology* **2018**, *154*, 1258.

[41] A. Treyer, A. Müsch, *Compr. Physiol.* **2013**, *3*, 243.

[42] H. Bäckdahl, G. Helenius, A. Bodin, U. Nannmark, B. R. Johansson, B. Risberg, P. Gatenholm, *Biomaterials* **2006**, *27*, 2141.

[43] S. N. Bhatia, G. H. Underhill, K. S. Zaret, I. J. Fox, *Sci. Transl. Med.* **2014**, *6*, 245sr2.

[44] A. J. Benítez, J. Torres-Rendon, M. Poutanen, A. Walther, *Biomacromolecules* **2013**, *14*, 4497.

[45] A. J. Benítez, A. Walther, *J. Mater. Chem. A* **2017**, *5*, 16003.